



Gazi University

**Journal of Science**

PART A: ENGINEERING AND INNOVATION

<http://dergipark.org.tr/gujisa>

## Illumination Response of Impedance Properties of Al/Gr-PVA/p-Si (MPS) Device

Dilan ATA<sup>1\*</sup> Muzaffer BALBAŞI<sup>1</sup> Adem TATAROĞLU<sup>2</sup> <sup>1</sup>Gazi University, Faculty of Engineering, 06570, Ankara, Türkiye<sup>2</sup>Gazi University, Faculty of Science, 06560, Ankara, Türkiye

Keywords	Abstract
Gr Doped PVA Illumination Admittance Basic Electrical Parameters	Admittance measurements including capacitance (C) and conductance (G) of Al/Gr-PVA/p-Si (MPS) device were made at 500 kHz and under dark and 200 mW/cm <sup>2</sup> conditions. The illumination response on the electric characteristics of the device was investigated using the C-2-V characteristics. It was observed that the electronic parameters of the device changed depending on the illumination conditions. The doping concentration, Fermi energy and barrier height were obtained using the C-2-V data. The surface state (N <sub>ss</sub> ) was also obtained using capacitance data. The results show that the device can be used as a photocapacitor.
Cite	
Ata, D., Balbaşı, M., & Tataroğlu, A. (2023). Illumination Response of Impedance Properties of Al/Gr-PVA/p-Si (MPS) Device. <i>GU J Sci, Part A, 10(1)</i> , 89-96.	
Author ID (ORCID Number)	Article Process
D. Ata, 0000-0001-9670-3138	<b>Submission Date</b> 18.11.2022
M. Balbaşı, 0000-0003-0424-3424	<b>Revision Date</b> 24.11.2022
A. Tataroğlu, 0000-0003-2074-574X	<b>Accepted Date</b> 29.11.2022
	<b>Published Date</b> 20.03.2023

### 1. INTRODUCTION

Graphene (Gr) is one of the most promising materials due to its outstanding electric, optic, mechanic and thermal characteristics, such as strong electrical conductivity, high electron mobility, good flexibility and excellent chemical/thermal stability (Castro Neto et al., 2009; Sadasivuni et al., 2015; Wang et al., 2019). Graphene is extensively used in many electronic and optoelectronic device applications, which include field-effect transistors, energy storage devices like supercapacitors, flexible displays, sensors, photodetectors, and solar cells (Castro Neto et al., 2009; Bin Mohd Yusoff, 2015; Sadasivuni et al., 2015; Sang et al., 2019; Wang et al., 2019). Graphene is also an important material for transparent conductive electrodes. Graphene films can be grown by various methods including the chemical vapor deposition, pulsed laser deposition and electrochemical exfoliation of graphite.

Polymeric material has various characteristics such as easy processing, high-dielectric strength, light-weight, fracture tolerance, good chemical resistance and low manufacturing cost. PVA (Polyvinyl alcohol) is an easily produced polymer. PVA may be prepared by electro-spinning and sol-gel spin coating techniques. PVA has physicochemical properties, including good thermal stability, good flexibility, and good film forming (Finch, 1973; Ben Halima, 2016; Jafar Mazumder et al., 2019).

PVA has low electrical conductivity and becomes conductive with the addition of suitable dopant material (Bulinski, 2021). In addition, polymer-based dielectrics is often used to insulate electrical devices. Especially, dielectric polymers are preferred for charge-storage applications (Hashim, 2010). Pure polymers have generally a low dielectric constant. Polymer-based capacitors have important advantages like low dielectric loss, high breakdown strength, and easy production.

If a device is illuminated by light, the electron/hole pairs occur in depletion region (Wood, 1994). As light intensity increases, more carriers are formed in the depletion region. In other words, the number

\*Corresponding Author, e-mail: [dilan.savasturk@gazi.edu.tr](mailto:dilan.savasturk@gazi.edu.tr)

of these pairs is related to the photon energy. Also, the light-induced current is a result of the electron-hole pairs.

In this paper, we investigated illumination effect on electrical properties of the metal/polymer/semiconductor (MPS) device. The device was characterized under dark and 200 mW/cm<sup>2</sup> conditions. Admittance measurements (C and G) were also made at a constant frequency of 500 kHz. The device parameters were calculated for dark and illumination intensity.

## 2. MATERIAL AND METHOD

Boron-doped p-Si semiconductor wafer with 2-inch diameter, (100) orientation and 300 μm thickness was used as substrate. Before the Al/Gr-PVA/p-Si device were fabricated, Si was cleaned in an ultrasonic cleaner using chemical solvents. Detailed information about the formation of the Gr-PVP interlayer was given in the previous study (Ata et al., 2022).

The device was illuminated by a solar simulator (Newport/Oriel) with an AM 1.5G filter, which was only suitable for wavelengths between 400 and 700 nm. Admittance measurements of the device were made using HP 4192A at 500 kHz and under the dark and constant illumination conditions of 200 mW/cm<sup>2</sup>. Both capacitance and conductance were also measured using an alternating signal with a voltage amplitude of 100 mV.

## 3. RESULTS AND DISCUSSION

The complex admittance,  $Y$ , of parallel circuit (parallel connected C and G) is defined as,

$$Y(\omega) = G_p(\omega) + i\omega C_p \quad (1)$$

here  $G_p$  and  $C_p$  are the parallel conductance and capacitance, respectively. Both depend on frequency. At the same time, the complex impedance  $Z$  is equal to  $1/Y(\omega)$ . Admittance spectroscopy is a powerful technique used to investigate electrical and dielectric characteristics and ac behavior of electronic devices. Capacitance-voltage (C-V) measurements are one of the most basic electrical measurements for electronic devices. A varying dc voltage and ac small signal voltage with  $V(t)=V_0 \sin(\omega t)$  are applied across the device. The capacitance changes with frequency of the ac signal. At higher frequencies, the interface traps do not respond to ac signal and contribute to capacitance.

Figure 1 demonstrate the C-V plots. The measurements performed at a fixed frequency of 500 kHz showed that the capacitance value against the potential changes with increasing illumination intensity. When the illumination intensity per unit area is increased, capacitance values 'C' increases distinguishable. (Singh, 2003; Hashim, 2010; Tan et al., 2017; Tataroğlu et al., 2020; Buyukbas Ulusan et al., 2021; Al-Sehemi et al., 2022; Karataş & Yumuk, 2022).

These results confirm that the device exhibits photo-capacitive behavior, which is related to the photo-generated charges. The charge carriers are generated under illumination and accumulated at the interface. In addition, experimental measurements show that certain peaks for capacitance occur in the depletion region. These peaks are due to the distribution of deep traps in the band gap and interface states. As illumination intensity increases, the peak positions shift towards the lower voltages.

Figure 2 shows conductance-voltage ( $G/\omega$ -V) plots as a function of applied voltage. Similarly, experimental results adapted to a fixed frequency value at 500 kHz show that the conductivity value measured against the potential also changes with increasing illumination intensity. In other words, The  $G/\omega$ -V curve shows the conductance value rises with an increase in light intensity. The change in photo-conductance can be attributed to an increase in the number of photo-generated electrons with illumination intensity.

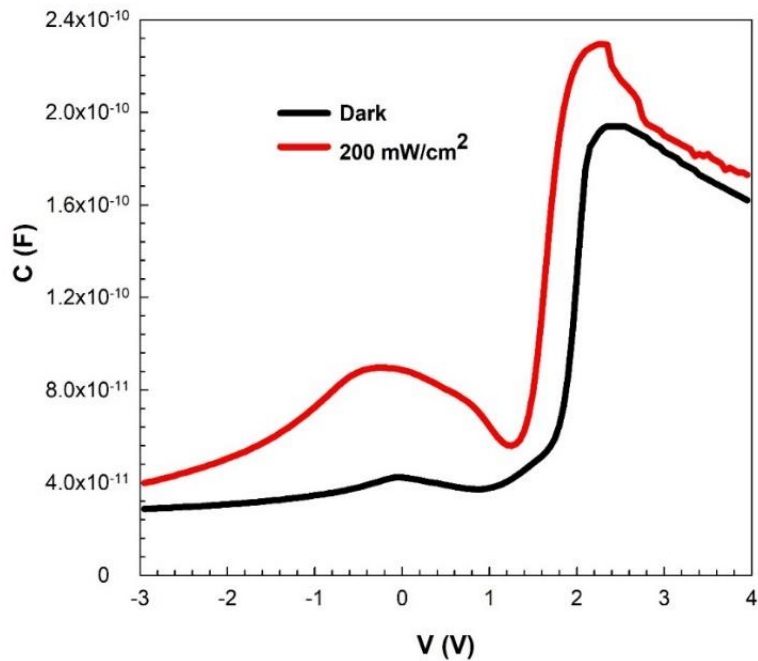


*Figure 1. C-V plots at 500 kHz*

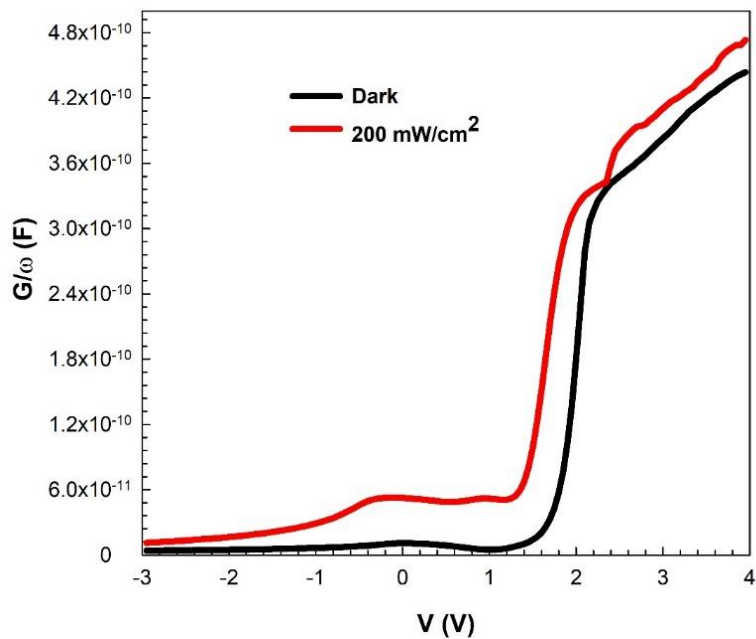


*Figure 2. G/omega-V plots at 500 kHz*

In practice, the admittance measurement is typically performed using an impedance analyzer, which is a specialized piece of test equipment that can measure the impedance of a circuit over a specific range of frequencies. The impedance measurement can then be converted to admittance, and the resistance can be calculated using the appropriate equations. Admittance measurements are used to calculate the resistance of a circuit in series. In a circuit with only resistive elements, the admittance is directly proportional to the conductance, which is the reciprocal of resistance. Hence, the resistance of a circuit can be calculated as the reciprocal of the conductance, which can be obtained from the admittance measurement.

All semiconductor devices contain series resistance parameter that affects their current-voltage (I-V) capacitance/conductance-voltage (C/G-V) characteristics and performance. Series resistance is mainly equal to the sum of the rectifier/ohmic contact resistances and the of the bulk resistance of semiconductor. The conductance method was used to extract series resistance ( $R_s$ ) of the prepared device (Nicollian & Goetzberger, 1967). The  $R_s$  value was calculated using the following expression,

$$R_s = \frac{G_m}{G_m^2 + (\omega C_m)^2} \quad (2)$$

Series resistance was calculated from admittance measurements. Figure 3 demonstrates  $R_s$ -V plots. It is seen that the increase in illumination intensity causes an increase in the series resistance in depletion region. Besides, the  $R_s$ -V plots indicate a peak along depletion region. This peak comes from interface traps. This peak position shifts towards the lower positive voltage with illumination.

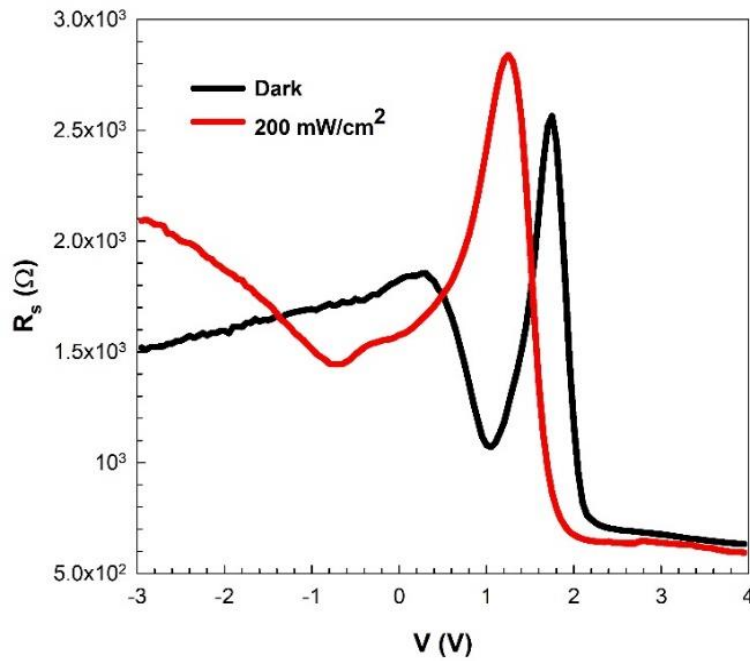


**Figure 3.**  $R_s$ -V plots at 500 kHz

The capacitance of depletion region of semiconductor devices is defined as: (Nicollian & Goetzberger, 1967; Sze, 1981; Nicollian & Brews, 1982; Tataroğlu & Altındal, 2006; Kim, 2016; Lambada et al., 2020),

$$C^{-2} = 2(V_0 + V)/(q\varepsilon_s\varepsilon_0A^2N_A) \quad (3)$$

The plot of  $C^{-2}$  versus  $V$  should yield a straight line. The diffusion potential ( $V_D=V_0+kT/q$ ) and acceptor concentration ( $N_A$ ) can be derived from the intercept-slope of the straight line of  $C^{-2}$ - $V$  plot. Here,  $E_F$ ,  $E_m$ ,  $\Delta\Phi_B$  and  $W_D$  represent the Fermi energy level, the maximum electric field, the image force barrier lowering and the depletion-layer width, respectively. Their values were commonly calculated using the following equations,

$$E_F = \frac{kT}{q} \ln\left(\frac{N_V}{N_A}\right) \quad (4)$$

$$E_m = \left[ \frac{2qN_A V_0}{\epsilon_s \epsilon_0} \right]^{0.5} \quad (5)$$

$$\Delta\Phi_B = \left[ \frac{qE_m}{4\pi\epsilon_s\epsilon_0} \right]^{0.5} R_s = \frac{G_m}{G_m^2 + (\omega C_m)^2} \quad (6)$$

$$W_D = \sqrt{\frac{2\epsilon_s\epsilon_0 V_D}{qN_A}} \quad (7)$$

In addition, the barrier height  $\Phi_B$  is given by,

$$\Phi_B = V_D + E_F - \Delta\Phi_B \quad (8)$$

Figure 4 shows  $C^{-2}$ -V plots of the device as a function of the reverse bias for dark and 200 mW/cm<sup>2</sup> conditions. The relationship between  $C^{-2}$  and V should be linear. It is clear that these plots indicate a straight line at a large reverse voltage. Also, it is observed that  $C^{-2}$  increases linearly with increase in the reverse applied voltage. The linearity of  $C^{-2}$ -V plots indicates that the interface states cannot follow the ac signal at 500 kHz.

The electrical parameters of the device extracted from Equations (4-8) have been given in Table 1. The  $\Phi_B$  and  $W_D$  values under light are smaller than values in dark. The barrier height is affected by the distribution of charge at the depletion region. The device exhibits a photovoltaic behavior since the main electrical parameters are affected by illumination. The reason was attributed to the fact that the applied illumination generates more free carriers in the valance band, which absorb energy and easily jump to the conduction band under illumination conditions.

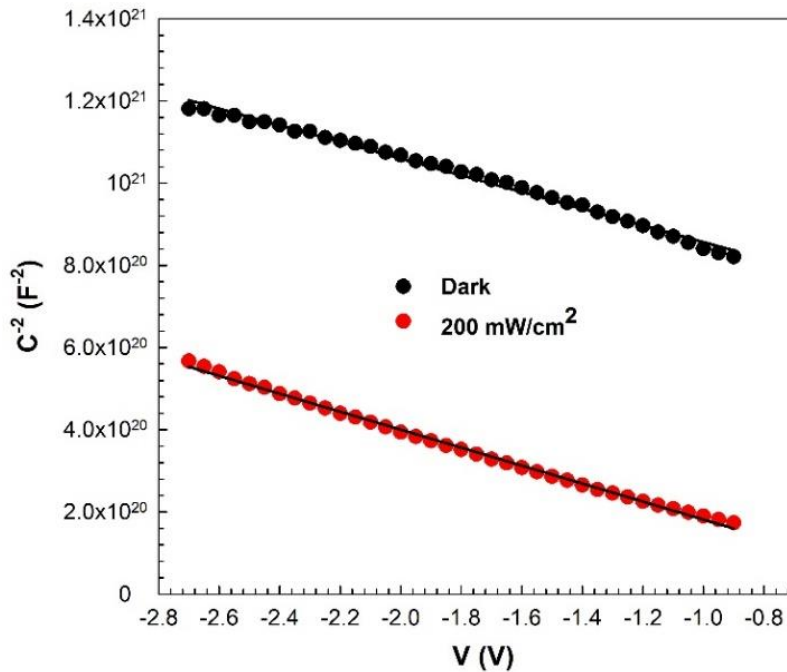


**Figure 4.**  $C^{-2}$ -V plots at 500 kHz

**Table 1.** Some electrical parameters of the MPS structure

<b>P</b> (mW/cm <sup>2</sup> )	<b>V<sub>D</sub></b> (eV)	<b>N<sub>A</sub></b> (cm <sup>-3</sup> )	<b>E<sub>F</sub></b> (eV)	<b>E<sub>m</sub></b> (V/cm)	<b>ΔΦ<sub>B</sub></b> (eV)	<b>Φ<sub>B</sub></b> (eV)	<b>W<sub>D</sub></b> (cm)
0 (Dark)	0.644	9.35x10 <sup>14</sup>	0.274	1.33x10 <sup>4</sup>	12.7.x10 <sup>-3</sup>	0.905	9.48x10 <sup>-5</sup>
200	0.356	8.88x10 <sup>14</sup>	0.275	0.95x10 <sup>4</sup>	10.8x10 <sup>-3</sup>	0.621	7.23x10 <sup>-5</sup>

The C-V measurements play an important role in the calculation of the interface state density ( $N_{ss}$ ). The voltage dependence profile of illumination-induced surface states between organic interlayer and semiconductor was extracted based on high-low C-V method (Sze, 1981; Brews & Nicollian, 1984; Pandey & Kal, 1998). At high frequencies ( $f \geq 500$  kHz), charges at interface traps are unable to react to the exterior ac signal, and therefore they cannot supply an excess capacitance to the real value of it. At low frequencies, the interface traps can follow the ac signal, thus, they may contribute the measured capacitance value.

The interface state density across the band gap was calculated from the formula below using dark instead of low and illumination instead of high defined in the capacitance method.

$$N_{ss} = \frac{1}{qA} \left\{ \left[ \frac{1}{C_{dark}} - \frac{1}{C_i} \right]^{-1} - \left[ \frac{1}{C_{ill}} - \frac{1}{C_i} \right]^{-1} \right\} \quad (9)$$

In Equation 9,  $C_i$  and  $A$  are the interlayer capacitance and rectifier contact area, respectively. The  $N_{ss}$ -V plot is given in Figure 5. This plot shows two peaks. The first peak is related to the density distribution of the surface state and the second peak is the result of series resistance.

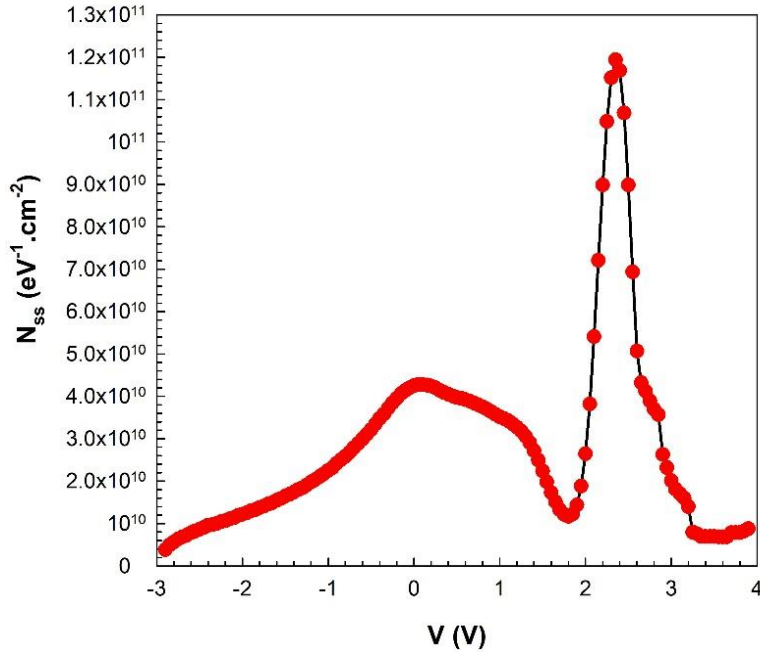


**Figure 5.**  $N_{ss}$ -V plot at 500 kHz

#### 4. CONCLUSION

This paper is concerned with the admittance measurements of the MPS structure under light illumination. These measurements were carried out at the constant frequency of 500 kHz under the dark and maximum constant illumination condition of 200 mW/cm<sup>2</sup>.

The results showed that the MPS structure exhibited photo capacitive behavior. Some parameters, including  $N_A$ ,  $E_F$ ,  $\Phi_B$  and  $W_D$  of the structure, were derived from the  $C^{-2}$ -V data. It was seen that these parameters were affected by the illumination. Besides, the  $N_{ss}$  versus V plot shows two distinctive peaks. These peaks indicate a special distribution of interface traps. In conclusion, the fabricated structure can serve as a photo capacitor in some specific optoelectronic applications.

#### CONFLICT OF INTEREST

The authors declare no conflict of interest.

#### REFERENCES

- Ata, D., Altindal Yeriskin, S., Tataroglu, A., & Balbasi, M. (2022). Analysis of admittance measurements of Al/Gr-PVA/p-Si (MPS) structure. *Journal of Physics and Chemistry of Solids*, 169, 110861. doi:[10.1016/j.jpcs.2022.110861](https://doi.org/10.1016/j.jpcs.2022.110861)
- Ben Halima, N. (2016). Poly(vinyl alcohol): review of its promising applications and insights into biodegradation. *RSC Advances*, 6(46), 39823-39832. doi:[10.1039/C6RA05742J](https://doi.org/10.1039/C6RA05742J)
- Bin Mohd Yusoff, A. R. (2015). *Graphene-based energy devices*. Wiley-VCH Verlag.
- Brews, J. R., & Nicollian, E. H. (1984). Improved MOS capacitor measurements using the Q-C method, *Solid-State Electronics*, 27(11), 963-975. doi:[10.1016/0038-1101\(84\)90070-4](https://doi.org/10.1016/0038-1101(84)90070-4)
- Bulinski, M. (2021). Metal doped PVA films for opto-electronics-optical and electronic properties, an overview. *Molecules*, 26(10), 2886. doi:[10.3390/molecules26102886](https://doi.org/10.3390/molecules26102886)
- Buyukbas Uluşan, A., Tataroglu, A., Altindal, S., & Azizian-Kalandaragh, Y. (2021). Photoresponse characteristics of Au/(CoFe<sub>2</sub>O<sub>4</sub>-PVP)/n-Si/Au (MPS) diode. *Journal of Materials Science: Materials in Electronics*, 32(12), 15732-15739. doi:[10.1007/s10854-021-06124-w](https://doi.org/10.1007/s10854-021-06124-w)
- Castro Neto, A. H., Guinea, F., Peres, N. M. R., Novoselov, K. S., & Geim, A. K. (2009). The electronic properties of graphene. *Reviews of Modern Physics*, 81(1), 109-162. doi:[10.1103/RevModPhys.81.109](https://doi.org/10.1103/RevModPhys.81.109)
- Finch, C. A. (1973). *Polyvinyl alcohol: Properties and applications*. Wiley.
- Hashim, A. A. (2010). *Polymer thin films*. InTech.
- Jafar Mazumder, M. A., Sheardown, H., & Al-Ahmed, A. (Eds.). (2019). *Functional polymers*. Springer International Publishing.
- Karataş, Ş., & Yumuk, M. (2022). Electrical characteristics of Al/(GO:PTCDA)/p-type Si structure under dark and light illumination: photovoltaic properties at 40 mW cm<sup>-2</sup>. *Journal of Materials Science: Materials in Electronics*, 33(14), 10800-10813. doi:[10.1007/s10854-022-08061-8](https://doi.org/10.1007/s10854-022-08061-8)
- Kim, H. (2016). Capacitance-voltage (C-V) characteristics of Cu/n-type InP Schottky diodes. *Transactions on Electrical and Electronic Materials*, 17(5), 293-296. doi:[10.4313/TEEM.2016.17.5.293](https://doi.org/10.4313/TEEM.2016.17.5.293)
- Lambada, D. R., Yang, S., Wang, Y., Ji, P., Shafique, S., & Wang, F. (2020). Investigation of Illumination Effects on the Electrical Properties of Au/GO/p-InP Heterojunction with a Graphene Oxide Interlayer. *Nanomanufacturing and Metrology*, 3(4), 269-281. doi:[10.1007/s41871-020-00078-z](https://doi.org/10.1007/s41871-020-00078-z)
- Nicollian, E. H., & Brews, J. R. (1982). *MOS physics and technology*. Wiley.
- Nicollian, E. H., & Goetzberger, A. (1967). The Si-SiO<sub>2</sub> Interface — Electrical Properties as Determined by the Metal-Insulator-Silicon Conductance Technique. *Bell System Technical Journal*, 46(6), 1055-1133. doi:[10.1002/j.1538-7305.1967.tb01727.x](https://doi.org/10.1002/j.1538-7305.1967.tb01727.x)

- Pandey, S., & Kal, S. (1998). A simple approach to the capacitance technique for determination of interface state density of a metal-semiconductor contact. *Solid-State Electronics*, 42(6), 943-949. doi:[10.1016/S0038-1101\(97\)00267-0](https://doi.org/10.1016/S0038-1101(97)00267-0)
- Sadasivuni, K. K., Ponnamma, D., Kim, J., & Thomas, S. (2015). *Graphene-based polymer nanocomposites in electronics*. Springer International Publishing.
- Sang, M., Shin, J., Kim, K., & Yu, K. J. (2019). Electronic and thermal properties of graphene and recent advances in graphene based electronics applications. *Nanomaterials*, 9(3), 374. doi:[10.3390/nano9030374](https://doi.org/10.3390/nano9030374)
- Singh, J. (2003). *Electronic and optoelectronic properties of semiconductor structures*. Cambridge University Press.
- Sze, S. M. (1981). *Physics of semiconductor devices*. Wiley.
- Tan, S. O., Uslu Tecimer, H., Çiçek, O., Tecimer, H., & Altındal, Ş. (2017). Frequency dependent C–V and G/ω–V characteristics on the illumination-induced Au/ZnO/n-GaAs Schottky barrier diodes. *Journal of Materials Science: Materials in Electronics*, 28(6), 4951-4957. doi:[10.1007/s10854-016-6147-0](https://doi.org/10.1007/s10854-016-6147-0)
- Tataroğlu, A., & Altındal, Ş. (2006). Characterization of current-voltage (I-V ) and capacitance-voltage-frequency (C-V-f) features of Al/SiO<sub>2</sub>/p-Si (MIS) Schottky diodes. *Microelectronic Engineering*, 83(3), 582–588. doi:[10.1016/j.mee.2005.12.014](https://doi.org/10.1016/j.mee.2005.12.014)
- Tataroğlu, A., Altındal, Ş., & Azizian-Kalandaragh, Y. (2020). Electrical and photoresponse properties of CoSO<sub>4</sub>-PVP interlayer based MPS diodes. *Journal of Materials Science: Materials in Electronics*, 31(14), 11665-11672. doi:[10.1007/s10854-020-03718-8](https://doi.org/10.1007/s10854-020-03718-8)
- Wang, J., Mu, X., & Sun, M. (2019). The thermal, electrical and thermoelectric properties of graphene nanomaterials. *Nanomaterials*, 9(2), 218. doi:[10.3390/nano9020218](https://doi.org/10.3390/nano9020218)
- Wood, D. (1994). *Optoelectronic semiconductor devices*. Prentice Hall.